Journal of Nuclear Materials 383 (2009) 270–273

Contents lists available at ScienceDirect

Journal of Nuclear Materials

journal homepage: www.elsevier.com/locate/jnucmat

Letter to the Editor

Effect of phosphorus on the mechanical behavior of a Zr–Nb alloy

Y.C. Choi [a], S. Ko [a], K.I. Chang [a], N.C. Cho [b], S.I. Hong [a,*]

[a] Department of Nano-materials Engineering, Chungnam National University, Taejon 305-764, Republic of Korea
[b] Tube Production Center, KNF, Taejon 305-309, Republic of Korea

ARTICLE INFO

Article history:
Received 9 June 2008
Accepted 22 September 2008

ABSTRACT

The flow stress of Zr–1.0Nb increased with the addition of 20 ppm phosphorous and the activation volume decreased with the addition of 300 ppm phosphorous at room temperature. The rate-controlling mechanism of the deformation of Zr–Nb–P is thought to be the dislocation-solute interaction in which the segregation of alloying elements affects the activation length. Less effective strengthening of phosphorous in Zr–Nb compared to sulphur was explained by a smaller electrostatic interaction between phosphorous atoms and dislocations.

1. Introduction

Many metals and alloys contain phosphorus and/or sulphur as impurities because they are present in nature combined with phosphorus and sulphur as metal sulphides, sulphates, phosphides and phosphates [1]. Phosphorus and sulphur have been known to cause the embrittlement in many alloys by reducing the boundary cohesive strength [2–6]. A surprising result that the thermal creep resistance can be improved drastically by the addition of sulphur as little as 10 ppm [7] has almost been unnoticed outside the nuclear industry and the nuclear-related academic community. The addition of 25 wt% ppm sulphur is known to be enough to reduce the creep rate of zirconium alloys by a factor of three at 400 °C [7,8]. Charquet [9] also reported that sulphur has an extremely beneficial effect on the steam corrosion resistance in zirconium alloys at 400 °C.

Recently Chang and Hong [10] reported that the flow stress of a Zr–Nb alloy increased by 65 MPa even at room temperature with the addition of sulphur as little as 20 ppm. They [10] observed the additive nature of sulphur strengthening in which the entire stress–strain curve shifted upward by the friction stress. Chang and Hong [10] and Ferrer et al. [8] could not find any sulphides despite extensive efforts to identify sulphide precipitates or particles. On the other hand, Hu et al. [11] observed sulphide and phosphide precipitation associated with carbon saturation in a Ti base alloy. Titanium and zirconium have the same HCP (hexagonal closed packed) structure and similar physical and chemical properties [10]. The sulphide/phosphide precipitation depended on the solution treatment temperature in a Ti alloy furnace-cooled after heat treatment [11]. The absence of sulphide in Zr–Nb alloys [7,9,10,12] may be due to the suppression of nucleation and growth of sulphide by quenching after high temperature heat treatment. Phosphorus and sulphur may behave similarly in Zr–Nb since they have the similar electronic structure (sulphur has two $3p_x$ electrons whereas phosphorus has one $3p_x$ electron) and the similar atomic radius. The primary objective of this study is to examine the effect of phosphorous on the mechanical behavior of a Zr–Nb alloy.

2. Experimental

Zr–1 wt% Nb alloys with no phosphorus addition and with various phosphorous contents (23 ppm, 312 ppm) were cast by vacuum arc melting. The addition of phosphorous was made by adding iron phosphide in the melt. The buttons were annealed (850 °C/1 h), β-quenched (from 1095 °C to water maintained at room temperature), hot-rolled at 580 °C annealed at 600 °C and cold-rolled into 1 mm thick plates with an intermediate heat treatment at 600 °C. The total reduction of the thickness during cold rolling was 75% with the final reduction of thickness equal to 30% after the intermediate heat treatment. Impurity contents of two Zr–1Nb alloys are summarized in Table. 1. Tensile testing was performed on cold-rolled specimens cut parallel to the rolling axis using a united testing machine (SFP 10). Strain jump tests were performed at room temperature and 300 °C to obtain the activation volume. In strain jump tests, the samples were initially strained at the strain rate of 10^{-4}/s and the strain rate was changed to 10^{-2}/s at the plastic strain of 0.01.

3. Experimental results and discussion

In Fig. 1(a–c), the optical micrographs (transverse section parallel to the rolling axis) of Zr–1.0Nb (a), Zr–1.0Nb–20 ppm P (b) and Zr–1.0Nb–300 ppm P (c) are shown. Equi-axed grain structure was observed and the addition of phosphorous was found to have no influence on the general microstructure. The grain size was

* Corresponding author. Tel.: +82 42 821 6595; fax: +82 42 822 5850.
E-mail address: sihong@cnu.ac.kr (S.I. Hong).

0022-3115/$ - see front matter © 2008 Elsevier B.V. All rights reserved.
doi:10.1016/j.jnucmat.2008.09.023

Table 1
Impurity contents of Zr–Nb–P alloys (ppm by weight)

	O	Fe	P	S
Zr–1Nb–20 ppm P	1100	630	23	<10
Zr–1Nb–300 ppm P	1000	870	304	<10

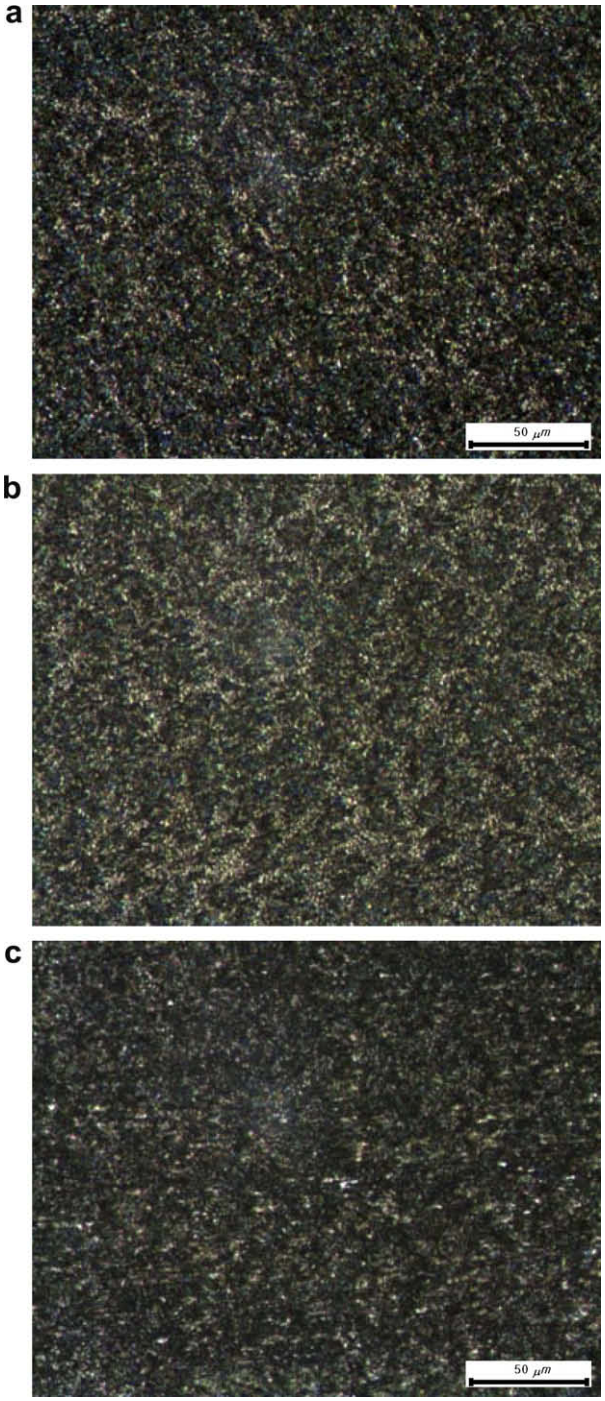

Fig. 1. Optical micrographs of as-rolled Zr–1.0Nb (a), Zr–1.0Nb–20 ppm P (b) and Zr–1.0Nb–300 ppm P (c).

~2.2 μm for all three alloys and no effect of phosphorous on the grain size was observed. X-ray diffraction pattern analysis did not display any peak from phosphorous containing compounds such as iron phosphide, zirconium phosphide and niobium phosphide, which is likely due to the low phosphorous content.

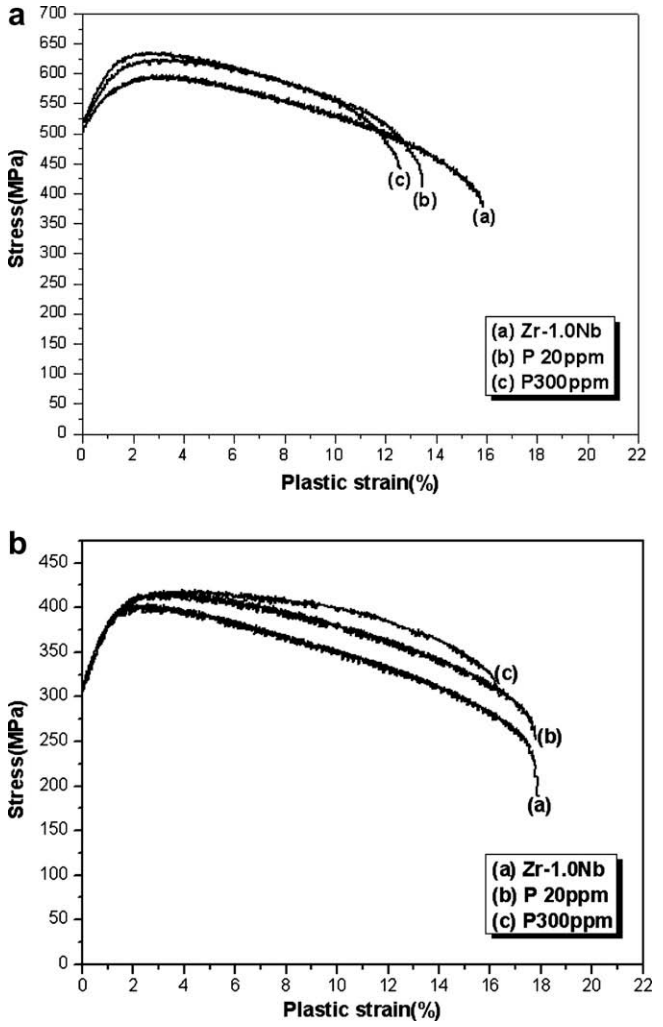

Fig. 2. Stress–strain responses of Zr–1.0Nb with various phosphorous contents at room temperature (a) and 300 °C (b).

The stress–strain responses of Zr–1.0Nb with no phosphorous and Zr–1.0Nb with 20 ppm and 300 ppm phosphorous at room temperature and 300 °C are shown in Fig 2(a) and (b) respectively. The flow stress increased by ~30 MPa at room temperature with the addition of 20 ppm phosphorous. With further increase of phosphorous content up to 300 ppm, a slight increase of the flow stress was observed. The elongation decreased with the increase of the phosphorous content. At 300 °C, the flow stress also increased, but by a smaller amount ~18 MPa with the addition of 20 ppm phosphorous and no appreciable change of the flow stress was observed with further increase of phosphorous. At 300 °C, however, the ductility was not reduced appreciably with the addition of phosphorous. An inappreciable increase of flow stress with increasing phosphorous content from 20 ppm to 300 ppm may be due to the limited solubility of phosphorous [7–10].

The strengthening effect of phosphorous in Zr–Nb alloy is less pronounced than that of sulfur. The phosphorous strengthening was observed both at room temperature and 300 °C in the present study as in Zr–Nb–S [10]. Chang and Hong [10] ascribed the sulphur strengthening at room temperature in their study to the high dislocation density of as-rolled Zr–Nb–S alloy. Alloys in the study of Ferrer et al. [8] were fully annealed after thermo-mechanical processing, and the dislocation density was low. Chang and Hong suggested that the diffusivity increases with the increase of dislocation density and

the effect of solute atoms could appear at lower temperatures in Zr alloys with higher dislocation density.

Fracture surfaces of Zr–1.0Nb (a), Zr–1.0Nb–20 ppm P (b) and Zr–1.0Nb–300 ppm P (c) after tensile testing at room temperature are displayed in Fig. 3(a–c). All alloys exhibited ductile fracture surfaces and no groove- or cleavage-like features [11] were observed, suggesting no significant detrimental effect of phosphorous in fracture of Zr–Nb alloys. In Zr–Nb–300 ppm P (Fig. 3(c)), secondary cracks were occasionally observed. The flow strength increase and good ductility in Zr–Nb–300 ppm P suggests that the secondary cracks were most likely formed in the final stage of fracture. Fig. 3(d) shows the fracture surface of Zr–Nb–300 ppm P at 300 °C and no secondary cracks were observed. The similar ductile fracture surfaces were observed at 300 °C for Zr–Nb and Zr–Nb-20 ppm P. The absence of groove- or cleavage-like features on the fracture surface is compatible with the observation that Zr–Nb alloys with 20 ppm phosphorous addition have no phosphide particles which may act as fracture paths as in Ti alloys [11]. The absence of large sulphides/phosphides in Zr–Nb–P ($P = 20$ ppm) and in Zr–Nb–S ($S < 300$ ppm) of other studies [7–10] is thought to be due to the rapid quenching of Zr–Nb alloys during thermomechanical processing. The solubility of sulphur in cold-worked Zr–Nb appears to be higher than that of phosphorous. The formation of phosphide/sulphide precipitates were reported to be influenced by solution treatment temperature, cooling rate and aging at intermediate temperatures in a Ti alloy [11]. For better strengthening effects of sulphur and phosphorous, the thermo-mechanical processing such as quenching and/or heavy-working which favors suppression of precipitation and/or dissolution of precipitates should be used.

In order to investigate the effect of phosphorous on the activation volume for deformation of Zr–Nb alloys, the activation volume for plastic flow was measured. The activation volume V^* associated with the deformation process has been obtained from the following equation [13,14]:

$$V^* = kT\partial \ln \gamma^* / \partial \tau = mkT \ln(\varepsilon_1^*/\varepsilon_2^*)(\sigma_1 - \sigma_2)$$

where k is the Boltzmann constant, γ^* is the shear strain rate, σ_1 and σ_2 are the applied shear stresses at the normal strain rates ε_1^* and ε_2^* and T is the absolute temperature. The shear stress τ was calculated from the normal flow stress σ, using the relation $\tau = \sigma/m$, where m is the Taylor factor. According to Luton and Jonas, m is assumed to be equal to 4 [15]. The activation volume, V^*, decreased from $\sim 147b^3$ to $\sim 127b^3$ where b is the Burgers vector with the addition of 300 ppm phosphorous at room temperature. The activation volume obtained at room temperature in Zr–1.0Nb–300 ppm P of the present study ($127b^3$) is a little larger than that ($80b^3$) observed by Chang and Hong [10] on similarly processed Zr–Nb–S containing 300 ppm sulphur.

Ferrer et al. [8] examined the effect of sulphur on the plastic deformation of Zr–Nb and tried to explain the origin of sulphur effect. Ferrer et al. [8] suggested that sulphur segregation at dislocation core could modify the core structure of dislocations, which would affect most of the dislocation properties including Peierls friction, cross slip, pipe diffusion and interaction with other impurities. However, for the modification of dislocation cores by sulphur to be an operative strengthening mechanism, the dislocation cores should be modified over a reasonable length of dislocations with the modified core structure maintained while they are in motion during deformation. It is questionable if the mobility of sulphur atoms is high enough to keep up with moving dislocations to maintain the modified dislocation core structure during deformation. In Ferrer's model, if the dislocations are liberated from the segregated sulphur atoms, the modified core structure

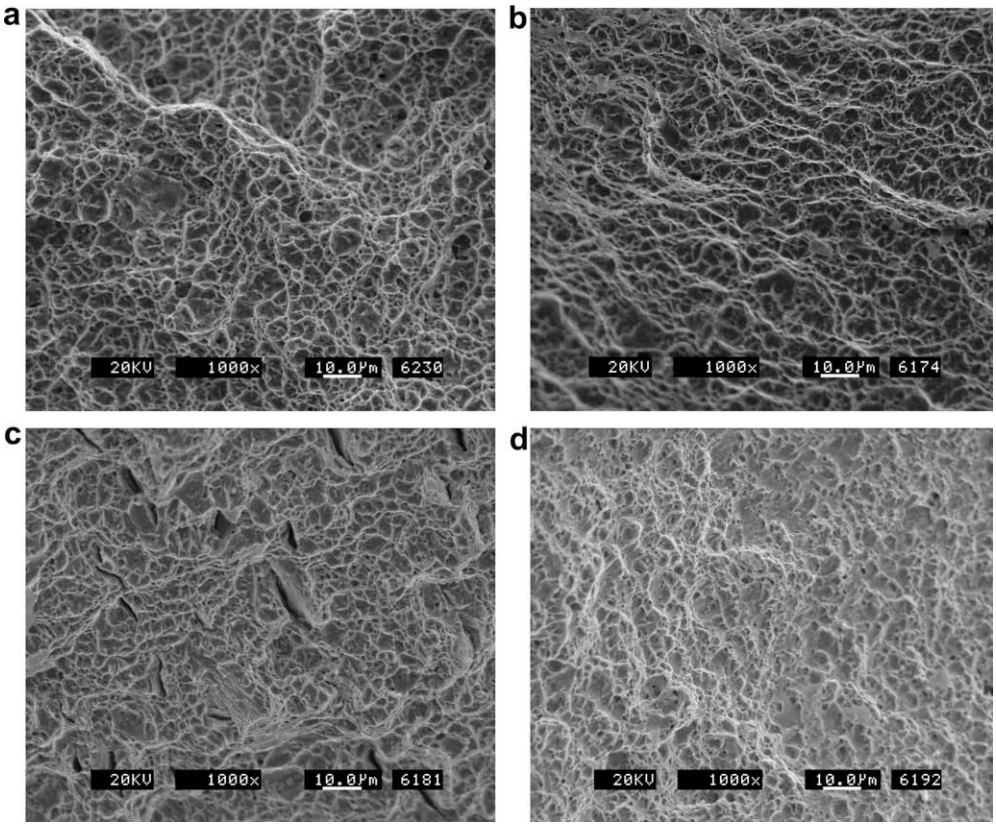

Fig. 3. Fracture surfaces of Zr–1.0Nb (a), Zr–1.0Nb–20 ppm P (b), Zr–1.0Nb–300 ppm P (c) after tensile testing at room temperature and Zr–1.0Nb–300 ppm P (d) at 300 °C.

would return to its original structure and the Peierls friction may not be appreciable.

Chang and Hong [10] suggested that the rate-controlling mechanism for the deformation of Zr–Nb and Zr–Nb–S alloys can best be explained by the dislocation interaction mechanism in which the segregation of alloying elements which affects the activation length of dislocations [12]. Kocks suggested that the activation length is affected by the segregated alloying elements although the maximum bulge length is limited by the spacing of forest dislocations. The segregation of sulphur or phosphorous atoms in addition to oxygen atoms [16–21] could decrease the activation volume by limiting the length of the activated bulge and enhance the strengthening effect. Dislocations can collect a significant number of solute atoms from its surroundings after being stopped by forest dislocations [12,16] at low temperatures.

The segregation of phosphorous atoms to dislocations in addition to oxygen atoms [18–21] in Zr–Nb–P alloy can result in the slight decrease of the activation volume and the increase of the strength as in Zr–Nb–S [10]. The reason why sulphur is more effective in strengthening of Zr–Nb alloy than phosphorous can be explained by the solution hardening theory. The solid solution hardening arises from the disturbing effects on dislocation motion [24]. The most important factors affecting dislocation motion in solution hardening are the size factor, the modulus factor and the electronic factor [23–26]. Although the size and modulus differences have been used extensively in many solution hardening models [25,26], Hutchison and Honeycombe [27] noted that solution hardening of silver alloys are related to the electronic influence of the solute atoms. Fleischer also noted that the local modulus change can be caused by the electronic effect [25,26].

Later, Morinaga and Kamado [22] found that both solution hardening and precipitation hardening of Al alloys can best be predicted by the size difference and the electronegativity difference between the matrix and solute atoms. Planken and Deruyttere [23] suggested that solution hardening should increase with electronegativity of the atom for a given size factor. The atomic radius of phosphorous (0.109 nm) is very close to that of sulphur (0.106 nm) and, therefore, the difference of strengthening due to sulphur/phosphorous addition can be linked with electronegativity difference between zirconium and sulphur or phosphorous. Since the electronegativity of sulphur, phosphorous and zirconium are 2.58, 2.19 and 1.33 respectively [28], the electronegativity difference between Zr and S is 1.25 and that between Zr and P is 0.86. Therefore, the electrostatic interaction due to the dipole creation between solute atoms and dislocation is greater in Zr–Nb–S than in Zr–Nb–P, resulting in a greater strengthening in Zr–Nb–S.

4. Conclusions

On the basis of the investigation of the effect of phosphorus on the strengthening and the activation volume, the following conclusions can be drawn:

1. The strength increased with the addition of phosphorous both at room temperature and 300 °C.
2. The activation volume decreased from $147b^3$ to $127b^3$ with the addition of 300 ppm phosphorous at room temperature. The activation volume obtained at room temperature in Zr–1.0Nb–300 ppm P ($127b^3$) is a little larger than that of similarly processed Zr–Nb–S–300 ppm sulphur ($80b^3$).
3. The elongation decreased with the increase of the phosphorous content, but all alloys containing phosphorous up to 300 ppm exhibited ductile fracture surfaces.
4. The rate-controlling mechanism of the deformation can be explained by the dislocation interaction mechanism in which the segregation of oxygen and phosphorous atoms affects the activation length of dislocations.
5. Less effective strengthening in Zr–Nb–P compared to similarly processed Zr–Nb–S can be linked to the smaller electrostatic interaction between solute atoms and dislocations due to a smaller electronegativity of phosphorous atoms.

Acknowledgement

The authors acknowledge the support from MOCIE (Ministry of Commerce, Industry and Energy), funded through Korea Nuclear Fuel Co. (2007).

References

[1] A.J. Stewart, M.W. Scimidt, Geophys. Res. Lett. 34 (2007) L13201.
[2] D. Bika, C.J. McMahon Jr, Acta Metall. Mater. 43 (1995) 1909.
[3] J.K. Heuer, P.R. Okamoto, N.Q. Lam, J.F. Stubbins, J. Nucl. Mater. 301 (2002) 129.
[4] Z.F. Hu, Z.G. Yang, Mater. Sci. Eng. A 383 (2004) 224.
[5] R.J. Haydock, Phys. C 14 (1981) 3807.
[6] R. Wu, A.J. Freeman, G.B. Olson, Science 265 (1994) 376.
[7] D. Charquet, J. Senevat, J.P. Marcon, J. Nucl. Mater. 255 (1998) 78.
[8] F. Ferrer, A. Barbu, T. Bretheau, J. Crepin, F. Willaime, D. Charquet, in: G.D. Moan, P. Rudling (Ed.), Thirteenth International Symposium on Zirconium in the Nuclear Industry, ASTM STP 1423, 2002, p. 863.
[9] D. Charquet, J. Nucl. Mater. 304 (2002) 246.
[10] K.I. Chang, S.I. Hong, J. Nucl. Mater. 373 (2008) 16.
[11] D. Hu, A.J. Huang, X.P. Song, X. Wu, J. Alloy Compd. 413 (2006) 77.
[12] U.F. Kocks, Metall. Trans. 16A (1985) 2109.
[13] H. Conrad, J. Met. 16 (1964) 582.
[14] S.I. Hong, K.W. Lee, K.T. Kim, J. Nucl. Mater. 303 (2002) 169.
[15] M.J. Luton, J.J. Jonas, Can. Metal. Quart. 11 (1972) 79.
[16] Z.S. Basinski, R.A. Foxall, R. Pascual, Scripta Metall. 6 (1972) 807.
[17] S.I. Hong, C. Laird, Acta Metall. Mater. 38 (1990) 1581.
[18] J.L. Snoek, Physica 8 (1941) 711.
[19] S.I. Hong, Scripta Mater. 44 (2001) 995.
[20] S.I. Hong, W.S. Ryu, C.S. Rim, J. Nucl. Mater. 120 (1984) 1.
[21] S.I. Hong, W.S. Ryu, C.S. Rim, J. Nucl. Mater. 116 (1983) 314.
[22] M. Morinaga, S. Kamado, Modelling Simul. Mater. Sci. Eng. 1 (1993) 151.
[23] J. van der Planken, A. Deruyttere, J. Mater. Sci. 4 (1969) 499.
[24] W.G. Johnston, J. Appl. Phys. 33 (1962) 2716.
[25] R.L. Fleischer, Acta Metall. 11 (1963) 203.
[26] R.L. Fleischer, Acta Metall. 9 (1961) 996.
[27] M.M. Hutchison, R.W.K. Honeycombe, Met. Sci. J. 1 (1967) 70.
[28] S. Ege, Organic Chemistry, 5th Ed., Houghton Miffin Co., Boston, 2003. p. 27.